

# Mean Grain Size and Pore Effects on Ultrasonic Properties of WC–Fe–Ni and SiC–Fe–Ni Composites

İ.H. SARPÜN<sup>a,\*</sup>, V. ÖZKAN<sup>b</sup>, A. YÖNETKEN<sup>c</sup> AND A. EROL<sup>c</sup>

<sup>a</sup>Afyon Kocatepe University, Physics Dept., Afyonkarahisar, Turkey

<sup>b</sup>Muş Alparslan University, Physics Dept., Muş, Turkey

<sup>c</sup>Afyon Kocatepe University, Technical Education Faculty, Afyonkarahisar, Turkey

(Received January 26, 2012; revised version April 5, 2012; in final form February 26, 2013)

In this work, electroless nickel plating technique was used with WC–Fe and SiC–Fe powders. Plated powders were sintered at temperature ranging from 600 °C to 1100 °C under argon shroud in Phoenix microwave furnace. The mean grain size is determined by using three different techniques namely ultrasonic velocity, ultrasonic attenuation, and rate of screen heights of successive peaks according to the pulse-echo method by using a 2 MHz and a 4 MHz probes compared with the scanning electron microscopy images. In addition, the relative effects of porosity on ultrasonic attenuation and velocity in the WC–Fe–Ni and SiC–Fe–Ni composite samples are studied. It is seen that the ultrasonic velocity, the ultrasonic attenuation, the rate of screen heights of successive peaks have a linear relation with the mean grain size of samples. However, the correlation coefficients of porosity graphs have higher values than mean grain size graphs for the composite materials as expected. This indicates that porosity determines the ultrasonic velocity and attenuation for the composite samples.

DOI: [10.12693/APhysPolA.123.688](https://doi.org/10.12693/APhysPolA.123.688)

PACS: 43.35.Ae, 81.70.–q, 43.35.Zc

## 1. Introduction

Ultrasonic waves passing through the sample was affected by two basic quantities: pores and grains. The effects of these two quantities have varied depending on the internal structure of the sample, particle size and pores. Both particle size and porosity effects on ultrasonic wave propagation have been given by Thompson et al. [1]. This study shows that the porosity increases, both longitudinal and transverse velocity values decrease proportionally.

Investigation of relationship between ultrasonic quantities and mean grain size of samples are based on passing ultrasonic waves through the samples. Accordingly, mean grain sizes of the samples can be determined by using different ultrasonic quantities, ultrasonic attenuation, ultrasonic velocity and ultrasonic backscattering. The ultrasonic attenuation method has been used by several researchers [2–7]. By this method, the amplitudes of successive back-wall echoes' screen height are used to determine attenuation. Using Roney's model [2, 3], relation between ultrasonic attenuation and mean grain size can be determined. In the ultrasonic backscattering method, the frequency spectrum (frequency vs. amplitude plot) of two successive back-surface signals is obtained. From these spectra, attenuation coefficient at different frequencies is found out [8–11]. This method requires more so-

phisticated instrumentation than other ultrasonic methods. Also the backscattering method is used for relatively fine grained materials. Ultrasonic velocity depends on sample structure and scattering of ultrasonic waves in sample. Theoretical explanation of scattering ultrasonic waves in polycrystalline materials was carried out by Hirsekorn [12]. Experimental works have been realized by [13, 14]. Furthermore two other methods which are called ultrasonic relative attenuation (URA) that uses the first back-wall echo height [15] and graphic method that uses  $\log v dv/df - \log D\alpha$  graphs [16], respectively. In Ref. [16], the data of previous works have been used and results were compared with other ultrasonic methods.

The mechanical and physical properties of composites were investigated by several researchers with ultrasonic methods [17–22].

The carbides of tungsten, boron, silicon, titanium and tantalum have been used in various applications over the years. In general, they are very hard and possess excellent wear resistance as well as oxidation resistance [23]. Tungsten carbide cermets are the most important group of cutting tool materials because of their high hardness, refractoriness and wear resistance. In these composite materials, also known as hard metals, the WC particles are cemented together by a ductile metal/alloy binder, usually Co, using the conventional powder metallurgy technique [24]. Tungsten carbide (WC) is perhaps the earliest of the non-oxide ceramic materials that found widespread usage, primarily in the machinery industry as a hard metal for metal cutting and drilling. While WC is extremely hard and relatively tough for a ceramic, most

\*corresponding author; e-mail: [isarpun@gmail.com](mailto:isarpun@gmail.com)

of the WC-based products are actually metal–ceramic composites. SiC is one of the excellent reinforcements in metal matrix composites (MMCs), due to its unique properties of corrosion resistance, high modulus, and high strength up to high temperatures. Many MMCs have been investigated to improve the structural properties, e.g., Al, Mg and Ti based MMCs. It is widely recognized that the mechanical properties of MMCs are strongly dependent on the interfacial features between ceramic and metal phases. Because of the interface reaction of SiC with most of transition metals (such as Fe, Ni, Co) at high temperatures, the use of SiC as the reinforcements for these materials is limited [25].

The electroless plating is a widely-used coating method because it can coat electrically nonconductive materials, almost any surface that is stable in electroless plating solutions, and give a uniform thickness of coatings irrespective of the shape of the product to be plated [26]. Electroless nickel plating (EN) is an autocatalytic chemical reduction process in which the reducing agent is oxidized and  $\text{Ni}^{2+}$  ions are deposited (reduced) on the substrate surface [27]. Once the first layer of Ni is deposited, it acts as a catalyst for the process. For metals that catalyze the electrochemical reaction (e.g. Ni, Co, Cu, and Ag), a linear relationship between coating thickness and time is often obtained [28].

## 2. Theory

This study aims to determine the mean grain size of WC–Fe–Ni and SiC–Fe–Ni composite samples with three different methods using basically ultrasonic attenuation and ultrasonic velocity quantities. In addition, in these composite structures, the relation between ultrasonic quantities and porosity were examined.

### 2.1. Ultrasonic velocity technique

The relationship between ultrasonic velocity and grain size has been explained by Hirsekorn [12, 29]. Scattering theory in the Rayleigh region was expressed in terms of the wave number ( $k$ ), and the grain radius ( $a$ ) and calculation of longitudinal and transverse ultrasonic velocities in polycrystals have been given as a function of  $ka$  in Ref. [12]. Also, graphs of normalized velocity versus  $ka$  have been published. In these graphs, as the  $ka$  value changes, velocity first decreases, then increases and oscillates according to analysis presented in Ref. [14].

### 2.2. Ultrasonic attenuation technique

An ultrasonic wave loses its energy while it propagates through a material. We can measure this effect as a loss of signal amplitude on the screen of an ultrasonic flaw detector. Energy loss of a wave is mainly due to two mechanisms which are absorption (dislocation damping, magnetic domain damping, and thermo-elastic interactions, etc.) and scattering (occur at grain boundaries, voids, inclusions, second-phase particles, micro cracks and macro

cracks, etc.) processes. So, attenuation is a frequency-dependent coefficient and may be written as

$$\alpha(f) = \alpha_a(f) + \alpha_s(f), \quad (1)$$

where  $\alpha_a(f)$  and  $\alpha_s(f)$  are the absorption and scattering coefficients, respectively. The ultrasonic wave attenuation in the material is given by

$$A = A_0 \exp(-\alpha x), \quad (2)$$

where  $A_0$  is the initial amplitude of the wave,  $A$  is the amplitude at a local position  $x$ , and  $\alpha$  is the attenuation coefficient of the material. By measuring echo heights of successive peaks on the screen of ultrasonic flaw detector, attenuation coefficient of sample could be determined

$$\alpha = \frac{1}{d} 20 \log \frac{A_2}{A_1}, \quad (3)$$

where  $d$  is the thickness of sample,  $A_1$  and  $A_2$  are the successive echo heights. According to Roney's model [2] relation, which is applicable to grain size determination, between grain size and attenuation was given as

$$\frac{\bar{D}_2}{\bar{D}_1} = \frac{f_1}{f_2} = \frac{\alpha_1}{\alpha_2}. \quad (4)$$

### 2.3. Ultrasonic relative attenuation (URA) method

The theory of URA method was given by Palanichamy et al. [15]. By taking the natural logarithm of Eq. (2), one gets

$$\ln A = \ln A_0 - \alpha x. \quad (5)$$

If two different materials are used with the same ultrasonic wave energy input, one could write according to Eq. (2):

$$A_1 = A_0 \exp(-\alpha_1 x_1), \quad (6)$$

$$A_2 = A_0 \exp(-\alpha_2 x_2), \quad (7)$$

where  $\alpha_1$  and  $\alpha_2$  are attenuation coefficients and  $x_1$  and  $x_2$  are the local observation positions of the ultrasonic wave in the two specimens. After some algebra one can get

$$\ln \left( \frac{A_1}{A_2} \right) = \alpha_2 x_2 - \alpha_1 x_1. \quad (8)$$

One can also use Eq. (8) for two specimens of the same material but with different thickness.

All in these methods, reference samples should be used to plot reference graphs for determination of grain size of samples.

### 2.4. Apparent porosity

The theory of the effects of porosity on ultrasonic wave propagation has been studied extensively by some researchers. The apparent porosity values of studied samples are calculated according to Eq. (9) [30] and have been given in Table I:

$$\%P = \frac{m_{\text{wet}} - m_0}{m_{\text{wet}} - m_{\text{water}}} \times 100, \quad (9)$$

where  $m_{\text{water}}$  is the mass of the sample in the water.

TABLE I

Ultrasonic measurements, mean grain size and porosity of samples.

Composite	Sintering temperature [°C]	Ultrasonic velocity [km/s]	Ultrasonic attenuation [dB/mm]	Rate of peak heights	Mean grain size [ $\mu\text{m}$ ]	Porosity [%]
WC-Fe-Ni	600	1.680	8.65	0.160	12.0	12.916
	700	1.874	6.77	0.220	13.8	12.242
	800	1.977	5.43	0.310	14.5	11.441
	900	2.110	3.95	0.410	15.2	10.957
	1000	2.364	2.62	0.550	16.2	9.842
	1100	2.555	1.61	0.760	17.5	8.713
SiC-Fe-Ni	600	1.183	7.27	0.132	14.2	12.851
	800	1.297	4.19	0.267	15.0	11.788
	1000	1.530	1.54	0.622	17.4	9.205
	1100	1.663	0.69	0.792	18.0	8.439

### 3. Experiments

In this paper, we have used three ultrasonic methods which require reference samples to determine mean grain size. Instead of using reference samples, we have used two probes with two different frequencies, 2 MHz probe (Sonatest SLH2-10, T/R) to plot reference graphs and 4 MHz probe (Sonatest SLH4-10, T/R) to determine the mean grain size of particles in the sample by using Sonatest Sitescan 150 flaw detector.

Nickel chloride was used to obtain nickel for plating in the electroless plating. The powders used for the preparation of WC-Fe-Ni composite samples were 35% WC, 35% Fe and 30%  $\text{NiCl}_2 \cdot 6\text{H}_2\text{O}$  (nickel chloride) and SiC-Fe-Ni composite samples were 20% SiC, 50% Fe, and 30% Ni. For nickel coating bath, chemical compounds and ratios of samples were listed in Table II.

Chemical compounds and ratios of WC-Fe-Ni composites.

TABLE II

Compound	Mass [g]	
	WC-Fe-Ni	SiC-Fe-Ni
tungsten carbide (WC)	10.5	
silicon carbide (SiC)		6
iron (Fe)	10.5	15
$\text{NiCl}_2 \cdot 6\text{H}_2\text{O}$ (nickel chloride)	9	9
hydrazine hydrate ( $\text{N}_2\text{H}_4 \cdot \text{H}_2\text{O}$ )	20	30
pure water	80	70
temperature	95 °C	95 °C
pH	10	9

Prepared powders were placed in a 15 mm diameter mold and pressed using a hydraulic press at a pressure of 300 bar, then sintered at different temperatures under argon shroud in Phoenix microwave furnace.

Sintered samples were characterized using Leo 1430 VP model scanning electron microscopy (SEM). SEM images of WC-Fe-Ni and SiC-Fe-Ni samples are shown in Figs. 1 and 2, respectively.

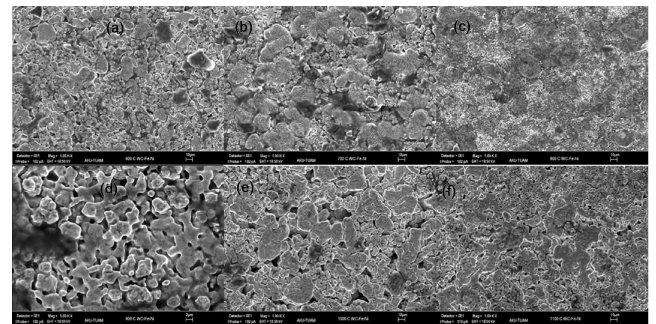


Fig. 1. SEM images of WC-Fe-Ni samples sintered at (a) 600 °C, (b) 700 °C, (c) 800 °C, (d) 900 °C, (e) 1000 °C and (f) 1100 °C.

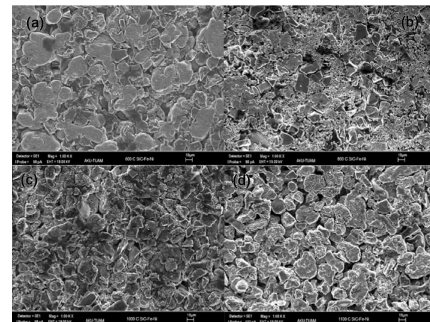


Fig. 2. SEM images of SiC-Fe-Ni composite samples sintered at (a) 600 °C, (b) 800 °C, (c) 1000 °C, (d) 1100 °C.

### 4. Results and discussion

The values measured by 2 MHz transducer were used to obtain reference graphs for three ultrasonic methods. The ultrasonic velocity, ultrasonic attenuation and rate of successive peak heights, porosity and the mean grain size of particles from SEM images were given in Table I.

The mean grain size increases with increasing sintering temperature that could be attributed to the increasing bonding between the grains. Also this is a good indicator

of correct sintering process. The increase in mean grain size results in decrease in sample volume that is decrease in porosity. These results are shown in Table I.

The relationship between ultrasonic velocity and porosity were given in Figs. 3 and 4, and between ultrasonic attenuation and porosity were given in Figs. 5 and 6 for WC-Fe-Ni and SiC-Fe-Ni composite samples by using Table I.

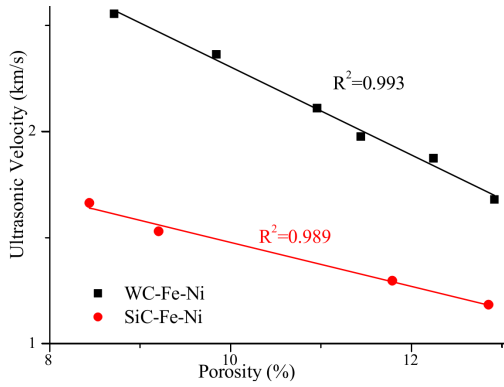


Fig. 3. Porosity-ultrasonic velocity graph of composite samples.

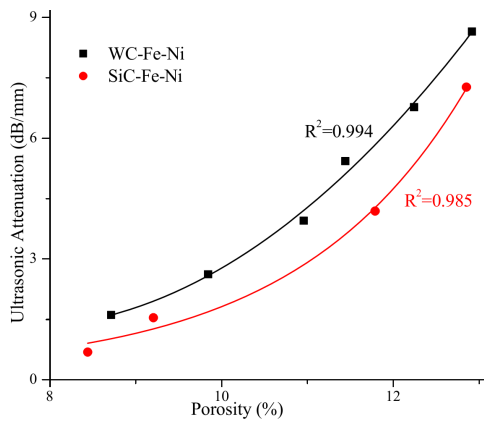


Fig. 4. Porosity-ultrasonic attenuation graph of composite samples.

The increase of mean grain size should result with the increased propagation speed of the wave since the wave will face less particle boundaries in the sample. These two results are as shown in Table I. Moreover, ultrasound speed increases with decreasing porosity that could be seen in Fig. 3.

Changes in the size or distribution of particles or porosity in a solid or liquid medium will affect the amplitude and frequency of scattered ultrasound. In porous ceramics/composites, the effect of the volume fraction of pores on ultrasonic parameters is expected to be much larger than that of the grain size. The decrease in the volume fraction of pores with increasing sintering temperature is expected to increase ultrasonic velocity and decrease ultrasonic attenuation.

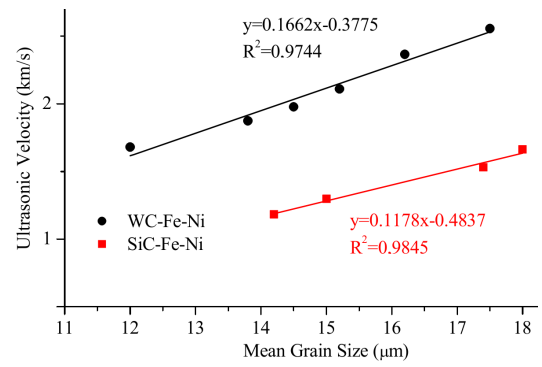


Fig. 5. Ultrasonic velocity-mean grain size graph of composite samples.

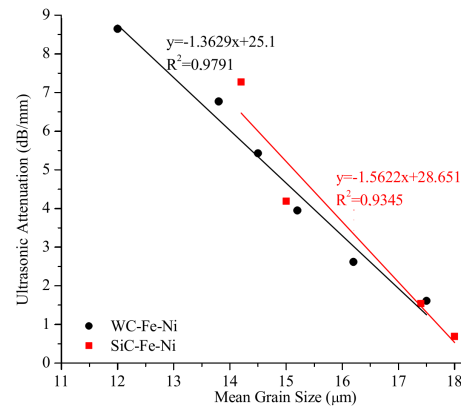


Fig. 6. Ultrasonic attenuation-mean grain size graph of composite samples.

Similarly increasing sintering temperature results in a decrease in particle boundaries in the sample which means less refraction and absorption with a smaller attenuation coefficient. This result is parallel to the findings presented in Fig. 4 and Fig. 6 with decrease in porosity and the mean grain size, respectively.

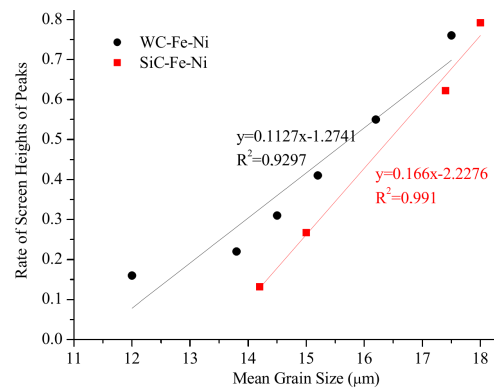


Fig. 7. Rate of peak heights-mean grain size graph of composite samples.

According to Table I, ultrasonic velocity-, ultrasonic attenuation-, and the rate of peak heights-mean grain size reference graphs were plotted and given in Figs. 5, 6 and 7, respectively.

The increasing mean grain size results in decreasing ultrasound speed which can be seen in Fig. 5.

The limiting duration of attenuation effect results in a decrease in peak height of the ultrasound wave and the ratio of successive peaks gets closer to one. This could be seen in Fig. 7 that relates the increase in the mean grain size of particles with the increase in screen peak heights.

Solid line in Figs. 5, 6, and 7 is a fit to experimental data for both WC-Fe-Ni and SiC-Fe-Ni samples. According to these fits, the mean grain size of samples was evaluated by using 4 MHz transducer's value. Ultrasonic velocity, ultrasonic attenuation and the rate of peak height values of 4 MHz probe and evaluated mean grain size are given for WC-Fe-Ni and SiC-Fe-Ni samples in Tables III and IV, respectively. According to Figs. 5, 6, and 7, our results show that the velocity of ultrasonic wave increases with decreasing porosity and the attenuation decreases with decreasing porosity.

Evaluated mean grain size of WC-Fe-Ni composite samples.

TABLE III

WC-Fe-Ni		600 °C	700 °C	800 °C	900 °C	1000 °C	1100 °C
experimental mean grain size [ $\mu\text{m}$ ]		12.0	13.8	14.5	15.2	16.2	17.5
Velocity	ultrasonic velocities 4 MHz [km/s]	2.016	2.121	2.260	2.438	2.604	2.834
	evaluated mean grain size [ $\mu\text{m}$ ] $y = 0.1178x - 0.4837$	14.4	15.0	15.9	16.9	17.9	19.3
	$\Delta$ (grain size) [ $\mu\text{m}$ ]	2.4	1.2	0.6	1.7	1.7	1.8
Attenuation	ultrasonic attenuation 4 MHz [dB/mm]	9.63	7.51	6.29	4.37	3.08	1.98
	evaluated mean grain size [ $\mu\text{m}$ ] $y = -1.3629x + 25.1$	11.4	12.9	13.8	15.2	16.2	17.0
	$\Delta$ (grain size) [ $\mu\text{m}$ ]	0.6	0.9	0.7	0	0	0.5
URA	rate of screen heights 4 MHz	0.13	0.21	0.24	0.38	0.5	0.63
	evaluated mean grain size [ $\mu\text{m}$ ] $y = 0.1127x - 1.2741$	12.5	13.2	13.4	14.7	15.7	16.9
	$\Delta$ (grain size) [ $\mu\text{m}$ ]	0.5	0.6	1.1	0.5	0.5	0.6

Evaluated mean grain size of SiC-Fe-Ni composite samples.

TABLE IV

SiC-Fe-Ni		600 °C	800 °C	1000 °C	1100 °C
experimental mean grain size [ $\mu\text{m}$ ]		14.2	15.0	17.4	18.0
Velocity	ultrasonic velocities 4 MHz [km/s]	1.267	1.535	1.998	2.139
	evaluated mean grain size [ $\mu\text{m}$ ] $y = 0.1662x - 0.3775$	14.9	17.2	21.1	22.3
	$\Delta$ (grain size) [ $\mu\text{m}$ ]	0.7	2.2	3.4	4.3
Attenuation	ultrasonic attenuation 4 MHz [dB/mm]	7.97	4.73	2.13	0.9
	evaluated mean grain size [ $\mu\text{m}$ ] $y = -1.5622x + 28.651$	13.2	15.3	17.0	17.8
	$\Delta$ (grain size) [ $\mu\text{m}$ ]	1.0	0.3	0.4	0.2
URA	rate of screen heights 4 MHz	0.109	0.234	0.52	0.739
	evaluated mean grain size [ $\mu\text{m}$ ] $y = 0.166x - 2.2276$	14.1	14.8	16.6	17.9
	$\Delta$ (grain size) [ $\mu\text{m}$ ]	0.1	0.2	0.8	0.1

The mean grain sizes both calculated and measured were plotted in Figs. 8 and 9 by using values from Tables III and IV.

All three methods used in this study gave comparable results as shown in Fig. 8 and Fig. 9. However, the ultrasonic velocity method has a relatively higher devi-

ation between the calculated and measured values than the other two methods used. On the other hand, both ultrasonic attenuation and URA methods show less than 10% deviation from the values obtained by the electron microscopy images. This deviation is up to 20% in ultrasonic velocity method.

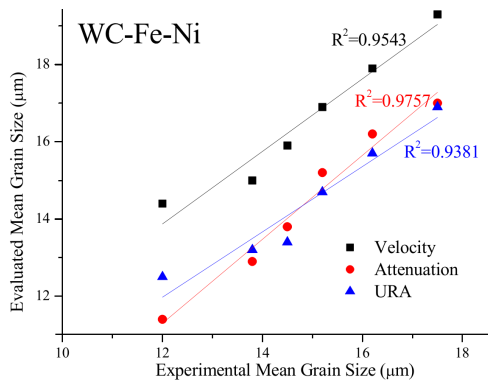


Fig. 8. Comparison of experimental and evaluated mean grain size of WC-Fe-Ni composites.

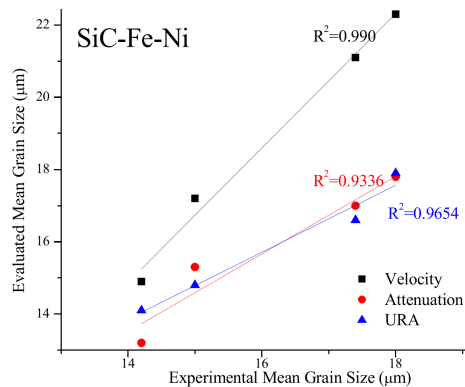


Fig. 9. Comparison of experimental and evaluated mean grain size of SiC-Fe-Ni composites.

## 5. Conclusion

The composites prepared from the powder mixtures having small particle size ratio (WC/Fe/Ni-SiC/Fe-Ni), appear to be clustered around the other powder particles boundaries in the form of a continuous network. The clustering become more evident with an increase in the amount of reinforcement and when examined the SEM images given in all figures, it can be seen that the structures have two types of pores, small and large. Particles are observed to form some necks with the other particles. It can be also seen that grain growth occurred due to bonding of particles to each other. We can say that the sintering temperature seems to play a more important role than sintering time.

The increase in the grain size is one of the changes due to the sintering process and is not the prime reason for the changes in the ultrasonic parameters. After careful measurement of the change in the volume fraction of pores/density of the specimens, the observed variations in the ultrasonic parameters correlate primarily with the pores and secondary with the grain size.

This work has shown that the ultrasonic velocity, the ultrasonic attenuation and the relative amplitude mea-

surements can be used to estimate mean grain size in composites.

WC-Fe-Ni samples have higher velocity than SiC-Fe-Ni samples as well as attenuation and peak height values.

## Acknowledgments

The authors wish to thank Birol Erol for helping in the electroless Ni plating and Afyon Kocatepe University, Technical Application and Research Center for their contribution to this work. This work has been supported by Afyon Kocatepe University Research grant number 06.FENED.11 and TUBITAK Research Project grant number 106T744.

## References

- [1] R.B. Thompson, W.A. Spitzig, T.A. Gray, in: *Review of Progress in Quantitative Nondestructive Evaluation*, Vol. 5B, Eds. D.O. Thompson, D.E. Chimenti, Plenum Press, New York 1986, p. 1643.
- [2] R.K. Roney, Ph.D. Thesis, California Institute of Technology, 1950.
- [3] J.B. Hull, C.M. Langton, S. Barker, A.R. Jones, *J. Mater. Process Technol.* **56**, 148 (1996).
- [4] E.E. Aldridge, *The Estimation of Grain Size in Metals, Non-Destructive Testing*, Oxford University Press, Oxford 1969.
- [5] B. Anfray, M. de Billy, G. Blanc, G. Quentin, *Proc. Ultrasonic Int.* **85**, 447 (1985).
- [6] D.K. Mak, *Can. Metall. Q.* **25**, 253 (1986).
- [7] D.W. Nicoletti, N. Bilgutay, B. Onaral, *IEEE Ultrason. Symp.* **2**, 1119 (1990).
- [8] D. Beecham, *Ultrasonics* **4**, 67 (1966).
- [9] K. Goebbels, P. Holler, *Ultrasonic Material Characterization*, Special Publication, National Bureau of Standards, Gaithersburg 1980, p. 67.
- [10] A. Hecht, R. Thiel, E. Neumann, E. Mundry, *Mater. Eval.* **39**, 934 (1981).
- [11] J. Sanjie, N.M. Bilgutay, *J. Acoust. Soc. Am.* **80**, 1816 (1986).
- [12] S. Hirsekorn, *New Procedures in Nondestructive Testing*, Springer, Berlin 1983, p. 265.
- [13] N. Grayali, J.C. Shyne, *Review of Progress in Quantitative NDE*, Vol. 4, Plenum Press, New York 1985, p. 927.
- [14] P. Palanichamy, A. Joseph, T. Jayakumar, B. Raj, *NDT&E Int.* **28**, 179 (1995).
- [15] P. Palanichamy, A. Joseph, A. Jayakumar, *Insight* **11**, 874 (1994).
- [16] L.R. Botvina, L.J. Fradkin, B. Bridge, *J. Mater. Sci.* **35**, 4673 (2000).
- [17] V. Özkan, İ.H. Sarpün, *Acta Phys. Pol. A* **121**, 184 (2012).
- [18] İ.H. Sarpün, V. Özkan, S. Tuncel, R. Ünal, *Int. J. Microstruct. Mater. Prop.* **4**, 104 (2009).
- [19] D. Ducret, R. El. Guerjouma, P. Guy, M. R'Mili, J.C. Baboux, P. Merle, *Elsevier Composites: Part A* **31**, 45 (2000).

- [20] A. Kazakewitsch, W. Riehemann, *Acta Phys. Pol. A* **122**, 516 (2012).
- [21] P.K. Rohatgi, S. Raman, B.S. Majumdar, A. Banerjee, *Elsevier Mater. Sci. Eng. A* **123**, 89 (1990).
- [22] N. Demirkol, F.N. Oktar, E.S. Kayali, *Acta Phys. Pol. A* **121**, 274 (2012).
- [23] A.W. Weimer, *Carbide, Nitride and Boride Materials Synthesis and Processing*, Chapman Hall, London 1997.
- [24] C.M. Fernandes, A.M.R. Senos, J.M. Castanio, M.T. Vieira, *Mater. Sci. Forum* **514-516**, 633 (2006).
- [25] S. Gang, W. Hailong, S. Fang, L. Kai, Z. Rui, *Key Eng. Mater.* **368-372**, 852 (2008).
- [26] M. Kang, E.D. Park, J.E. Yie, *Solid State Phenom.* **124-126**, 1145 (2007).
- [27] R. Taheri, Ph.D. Thesis, Department of Mechanical Engineering, University of Saskatchewan, Saskatoon 2003.
- [28] D. Baker, *Trans. Inst. Metal Finish* **71**, 121 (1993).
- [29] S. Hirsekorn, *J. Acoust. Soc. Am.* **72**, 1021 (1982).
- [30] B.K. Moh'd, *Electron. J. Geotechn. Eng.* **7B**, 7 (2002).